*Research Inventy: International Journal of Engineering And Science*
*Vol.13, Issue 2 (February. 2023), PP 119-126*
*Issn (e): 2278-4721, Issn (p):2319-6483, www.researchinventy.com*

# Design of a Transmitter Microstrip Antenna for The Detection of Cardiovascular Congestion

Rabia Toprak[1], Seyfettin Sinan Gultekin[2], and Dilek Uzer[2]
[1]*Department of Electrical-Electronics Engineering, Faculty of Engineering, Karamanoglu Mehmetbey University, 70100, Karaman, Türkiye.*
[2] *Department of Electrical-Electronics Engineering, Faculty of Engineering andNature Science, Konya Technical University, 42010, Konya, Türkiye.*

***Abstract:****Cardiovasculardisorders are one of the mostcommondeath causes in the world. The beginning of themtakes part in suddendeathsdevelop by depending on vascular occlusion. This paper, whichaims to eliminate the risksthat cause cardiovascular congestion such as arrhythmia and heartattack in itsearly stages, constitutes a basis. Cardiac occlusion maybedetected by a surgical intervention such as an angiogram or by a high-frequency diagnostic. By usingmicrostrip patch antennasthat have lots of usage in biomedical areas, a heart structure modelledismodeledwhilethereis congestion and not congestion in coronaryarteryvessels in Ansys' HFSS. First of all, the basic heart structure ismodeled by considering body dielectric values in the literature. The modeledheart structure issimulatedusing an antenna and differences in electricalfield values are evaluatedwith and without occlusion. Heart structure isprepared by usingphantompreparationmethods and S parameter values are comparedwith and without occlusion. The FR-4 with a thickness of 1.6 mm isselected. The operating frequency of the antennais 2.45 GHz. The microstripantenna structures canbeused in cardiovascular congestion as a result of different values in the parametersobtained.*
***Keywords:****Microstrip patch antenna, Biomedical antenna, Heart disease, Coronary artery, HFSS.*

---

Date of Submission: 12-02-2023 Date of Acceptance: 26-02-2023

---

## I. INTRODUCTION

Especiallyfor health systems, when it is necessary to stay and live at home, the importance of biomedical technologies increases. Wireless Body Area Network (WBAN) is an alternative for these situations [1]–[3]. Wearable and implantable antenna technologies are candidates for WBAN applications [4]–[6]. WBAN uses systems that there are transceiver and receiver antennas, biosensor and etc. So, information can quickly transfer from a system to another one. And concerned health worker can easily read, use and evaluate the necessary information.

Death causes arising from the circulatory system have the biggest ratio in Turkey and the world. Heart disorders have the biggest share in this ratio. According to a work made by Turkey Statistical Institution in 2019, in the death causes and rates, the biggest ratio is from heart disorders [7].

One of the most important reasons for the occurrence of heart disease is the congestion in the cardiovascular. Due to reasons such as living conditions, stress, unbalanced nutrition, deposits that are called fat particles or cholesterol are formed on the walls of the heart vessels. These deposits gradually increase over time, resulting in increased cardiovascular congestion rates. As a result, the heart cannot be fed sufficiently, and people are lost their lives because of sudden rhythm disorder or heart attack. Cardiovascular congestion could now be detected by surgical intervention called angiography or by using imaging systems with drug tomography. [8], [9]. In particular, the inability to display the level of congestion of the cardiovascular system with simple imaging systems increases the possibility of research for studies in the medical field.

The problem of congestion in the heart vessels occurs in the vessels feed the heart rather than the vessels feed the body. Vessels feed the body are veins carrying oxygen to the body. They are right coronary artery, left anterior descending coronary artery and circumflex artery. The left anterior descending artery feeds approximately two-thirds of the heart. This leads to undesired and vital loss as a result of the congestion of the vessels [8]. This situation can be prevented by detecting at the initial stage of the cardiovascular obstruction. There are several studies in the literature about the prevention of heart disease. A heart model, similar to the simulation models previously used for the detection of various disorders in the literature, is first modeled in this study to detect coronary artery congestion [10]–[12]. By considering a real heart structure, the heart structure is

modeled. In some literature, studies have been carried out to determine cardiac disorders by using antenna structures. However, in these studies, the modeling of S-parameters was performed with amount of water injected into the lung phantom structure, not congestion of the heart structure [13], [14]. In this study, the differences in both electric field values and S-parameter values are investigated.

The use of microstrip antenna structures for detection, treatment, and the prevention of various disorders in biomedical areas is still an area of study and continues to be developed [15], [16]. Some studies use the implanted stent structure as an antenna after opening the cardiovascular artery [17]. However, this study cannot be used at the early diagnosis stage for both the patient and the doctor as it requires surgical intervention. For this reason, the microstrip antenna structure is used for the predetermination of congestion in the heart vessels. Early detected coronary artery congestion is predicted to be useful in preventing various disorders such as heart attack and arrhythmia. The microstrip antenna structure is designed to operate at 2.45 GHz due to the ISM (Industrial, Scientific and Medical) frequency region. FR-4 material has chosen as the substrate.

In this paper, the heart structure has modeled in order to detect the above-mentioned disturbance in the initial stage and the microstrip antenna parameters are tested with congestion and without congestion in coronary artery vessels. Differences in electromagnetic field and S-parameter values in case of congestion in antenna parameters are shown with graphs. It is stated that the antenna performances, which are designed as both simulation and application, can be used in studies to detect coronary artery disorders.

## II. EXPERIMENTAL PROCEDURE

### 1. Modeled heart structure

The heart structure is modeled by considering a real human heart. The size of a person's heart is such as the size of fist [18]. Fig. 1 shows a real human heart and the heart structure modeled for simulation in this study such as another literature model for breast cancer in [19]–[25]. As with any material, the electrical properties of each biological tissue have different values. It is possible to find these values in the literature and it is also possible to find various phantom prescriptions giving these values in the literature [26], [27]. In this study, these recipes were used for phantom modeling. These values are given in Table 1. There are a variety of tissue models in the literature to identify different disorders [11], [28], [29].

**Figure1. A real human heart (right) and modelled heart structure (left).**

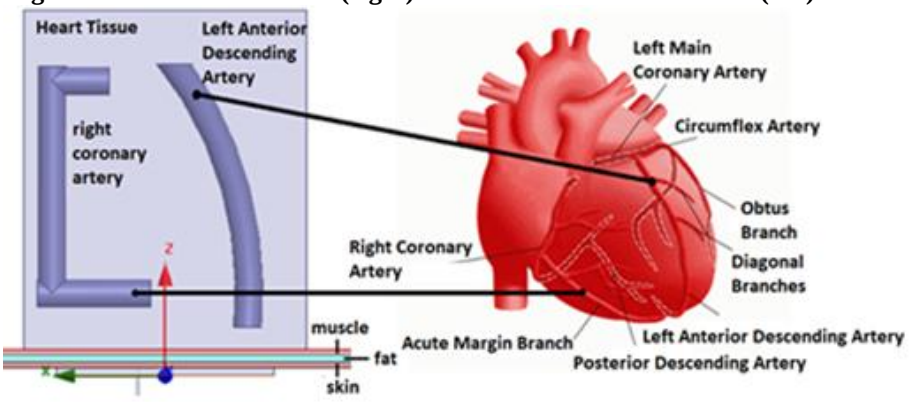


**Table1. Dielectric values and Recipes for biomedical tissues (for 2.45 GHz)**

| ***Tissue Type*** | $\varepsilon_r$ | Pure water (%) | Salt (%) | Sugar (%) | Flour (%) | Liquid Oil(%) |
|---|---|---|---|---|---|---|
| Skin | 38.00 | 50 | | 50 | | |
| **Fat** | **5.28** | **2.9** | **0.1** | | **67** | **30** |
| Muscle | 52.73 | 59.5 | 0.5 | 40 | | |
| **Heart** | **54.80** | **53.6** | **1.4** | **45** | | |
| Heart vessel | 42.50 | 53.6 | 1.4 | 45 | | |

The coronary arteries are modeled because of that, the heart structure is resembling a complex network of veins and it is difficult to model this structure during both the simulation and the application steps. The left anterior descending artery is likened to the true heart structure, and the right coronary artery is simulated by the letter 'C', thus modeling is performed [8]. The heart structure is placed on the skin, fat and muscle tissues. The reason for the absence of bone tissue is the lack of effect at microwave frequencies as mentioned in the literature [30]. In this study, skin, fat and muscle tissues are modeled with 1 mm thickness and 10x10 $mm^2$ area data. 6 cm length and 5x5 $cm^2$ area values were used in the heart structure. The heart structure here is chosen to be the

same as the heart of a real person. 5 mm diameter was selected in the cardiovascular structure. Real human heart vessel diameter values were obtained from [31].

In this study, the modeled heart structure is simulated in order to obtain the electromagnetic values of the antenna in Ansys HFSS software. In practice, phantom prescriptions are prepared and the experimental setup as in Fig. 2 is prepared. The block shape of setup is shown in Fig. 3. Here, fiberglass material receptacles are produced for the storage of tissue fluids.

**Figure 2. Prepared measurement device (left) normal view and bottom view (right).**

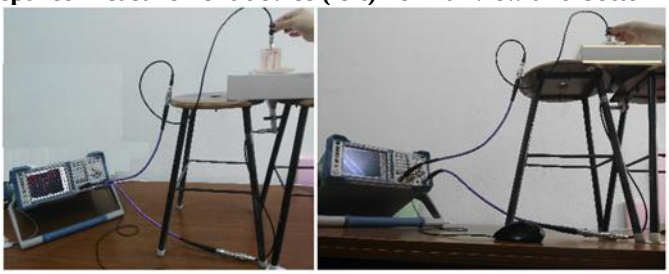

**Figure 3. The block shape of the measurement setup.**

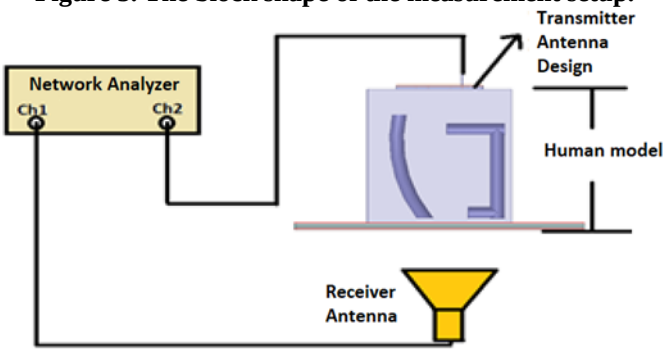


The sizes of these chambers are 10x10x2 $mm^3$ for the skin, 10x10x4 $mm^3$ for the fat, 10x10x6 $mm^3$ for the muscle and 5x5x6 $cm^3$ for the heart. A 5 mm diameter pipette is used for the heart vein. It is assumed that the cardiovascular is congested by placing a completely phantom in the pipette and the cardiovascular is healthy when there is no fat phantom. Since the tissue phantoms are liquid, the application is carried out in this way. In both the simulation and the application, the antenna is intended as an antenna structure used in the body and is constructed as a biosensor.

As a receiver horn antenna is used because of its high gain and from LRL Model 550B-SS Microwave Training Kit. Antenna measurements are implemented as far field radiation region expressed in [32]. Far field region distance must be longer than 13.6 mm. So it is selected as 2 cm.

## 2. Antenna Design

The antenna size is determined primarily from the following (1) and (2) [33]. When the calculated antenna values are considered, it is determined that the frequency is higher than 2.45 GHz. For this reason, an antenna structure with a frequency of 2.45 GHz resonance frequency has been formed by making the antenna patch diameter and patch width. The designed antenna and its dimensions are given in Fig. 4.

$$a = \frac{F}{\left\{1+{}^{2h}/_{\pi\epsilon_r F}\left[1+\ln\left(\frac{\pi F}{2h}\right)+1.7726\right]\right\}^{\frac{1}{2}}} (1)$$

$$F = \frac{8.791 \times 10^9}{f_r\sqrt{\epsilon_r}} (2)$$

where $f_r$ is operating frequency, $\epsilon_r$is dielectric constant of substrate, $h$is height of substrate and $a$ is radius of patch.

A circle with a diameter of 28.84 mm is drawn on the substrate material having a width of 38.3 mm. On the four-axis of the drawn circle, the circles of equal dimensions that have 16 mm diameter are placed. So, the resonant frequency is reduced to provide radiation at the desired 2.45 GHz region as shown in Fig. 5. This figure shows the simulation value in HFSS and the radiation data of the antenna measured using RS ZVL-13 vector network analyzer. The return loss simulation and measurement value of the antenna structure are -18 dB and

around -40 dB, respectively. As can be seen from the figure, the antenna gives more clear and better radiation values in the free space measurements. According to the simulation, the gain is 1.9 dB and input impedance value 50 Ω and 46.167 Ω for simulation and measurement, respectively.

**Figure 4. 2.45 GHz operating antenna structure dimensions and program output (left), produced part (right).**

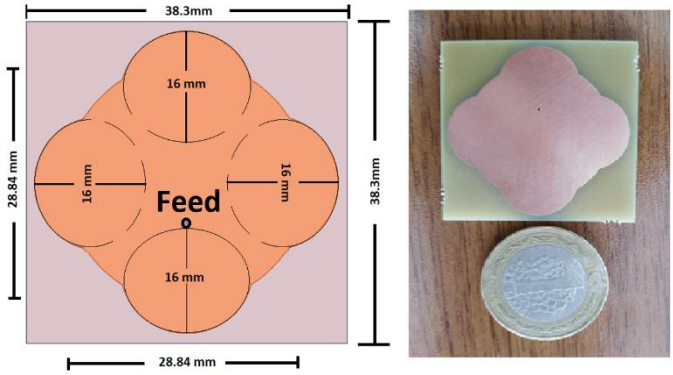


**Figure 5. Proposed antenna's return loss values after simulation and measurement.**


Simulations and measurements are both performed in free space. For implantable and similar biomedical applications, antenna dimensions are so important and when the proposed anten is compared with [22], [23], [34], [35], it has smaller dimensions. Once its gain is compared with [25], [36]–[40], it is bigger. Table 2 shows these differences. The efficiency of antenna is 0.99 for free space, 0.85 for heart structure without congestion and 0.94 for heart structure with congestion.

**Table 2. The comparison of proposed antenna with another literature antenna types.**

| Reference Number | Dimension (mm3) | Gain (dBi) |
|---|---|---|
| [29] | 1806 | - |
| [30] | 2112 | 4.59 |
| [32] | 80 | -20.8 |
| [34] | 120.69 | -22.7 |
| [44] | 2030 | 7.2 |
| [45] | 5471 | - |
| [46] | 695 | -15 |
| [47] | - | -16 |
| [48] | - | -29 |
| [49] | - | -19.9 |
| Proposed antenna | 1767 | 1.9 |

## III. SIMULATION, EXPERIMENTAL RESULTS AND EVALUATION

### 1. Simulation results

The antenna and the heart structure model designed in the HFSS are positioned on top of each other and simulated (Fig. 6). The material to be used as congestion is determined as fat tissue, and the right coronary artery and left coronary artery are covered with the congestion. The results of the measurements are evaluated for electromagnetic field values.

**Figure 6. The comparison of proposed antenna with another literature antenna types.**

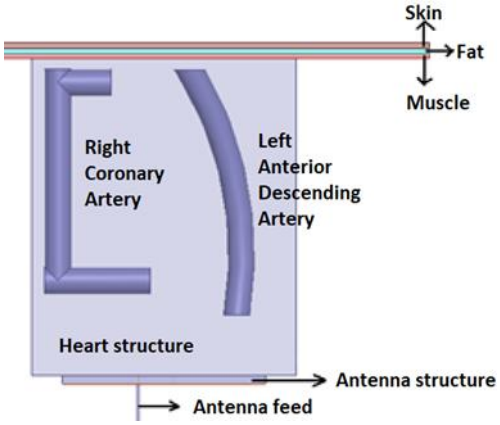


From HFSS, electric field values are obtained as data table. In order to calculate the electric field value in these graphs θ angle is changed between -180$^o$ and +180$^o$ and for φ = 0$^o$ and 90$^o$ values are got. For far field values, HFSS uses a spherical TEM wave with the following (3) [41].

$$\boldsymbol{E} = \eta_0 \sqrt{\frac{\mu_r}{\varepsilon_r}} \boldsymbol{Hxr} \quad (3)$$

Where $\eta_0$ is the intrinsic impedance of free space, $\eta_o = \sqrt{\mu_0/\varepsilon_0}$. E and H are electric and magnetic field values, respectively. r represents source points on the surface.

Electric field value unit is V/m. In HFSS, far field electric field data table value could receive as *rE* (mV), which is multiplied by the radial distance, *r* [41].

According to the theta angle, for Phi = 0$^o$, Fig. 7 shows that whether there are changes in the electric field values or not according to the state of congestion. In Fig. 8, there are variations of theta angle for Phi = 90$^o$. These changes are thought to be significant in early detection studies of cardiovascular congestion.

**Figure 7. Electrical field values depending on the theta angle of the antenna structure (Phi = 0$^o$).**

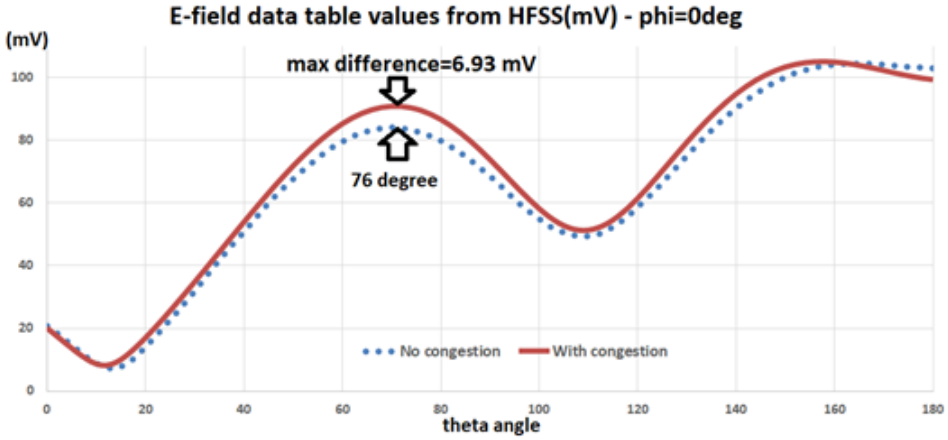

**Figure 8. Electrical field values depending on the theta angle of the antenna structure (Phi = 90°).**

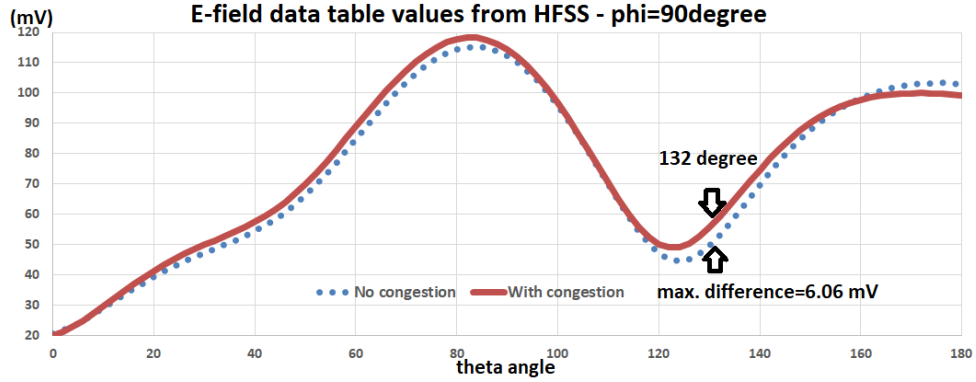


## 2. Experimental Results

The proposed antenna is implemented, and the system is prepared as described above. In this study, S-parameter values, also called scattering parameters, are measured in such a way that there is congestion and no congestion. Differences in $S_{11}$, $S_{12}$ and $S_{21}$ values are shown as a result of measurements. Fig. 9-11 show these graphics.

**Figure9. $S_{11}$ parameter measured from measurement process.**

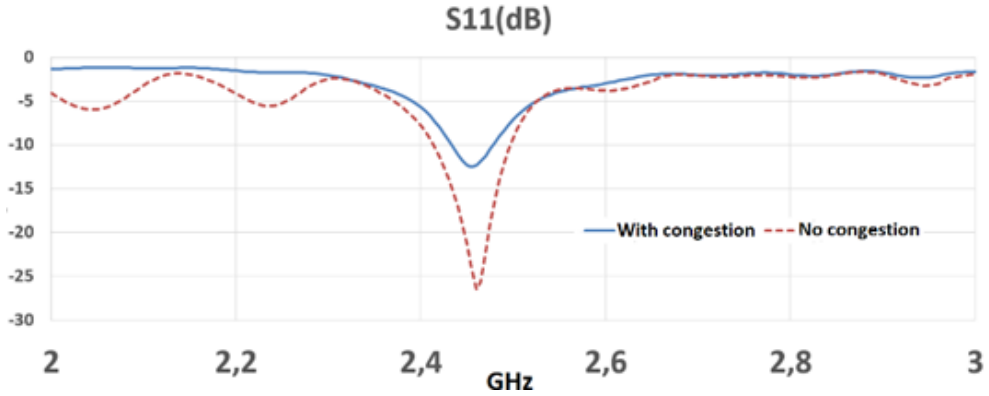


**Figure10. $S_{12}$ parameter measured from measurement process.**

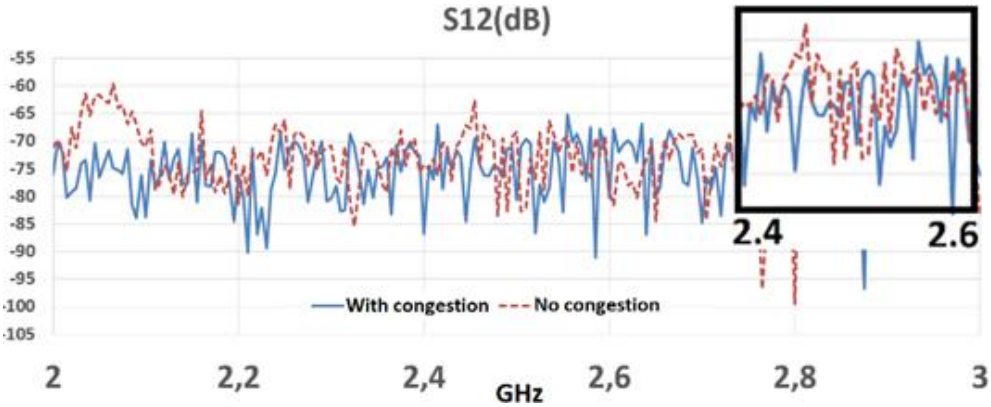


## 3. Evaluation

When the data obtained from the simulation and application results are examined, it can be seen that the designed antenna type can be used to determine cardiovascular congestion. The results obtained with and without congestion are the best examples of this. When the maximum values of the electric field in the case of congestion and no-congestion obtained are examined, the difference value for the antenna structure is 15 mV/m. The ratio of the absolute totals of the values in the graphic values obtained depending on the Theta angle

increased by 4.4% for φ= 0° and 2.8% for φ= 90° in case of congestion. If the application is in the frequency range of 2.4-2.5 GHz, the sum of the absolute values of $S_{12}$ decreases by 2% while the absolute value of $S_{21}$ decreases by 0.71%. At $S_{11}$, electric field values decrease about 17% while there is congestion in the vessels as seen in Figure 11, and at $S_{22}$ there is no change as expected.

**Figure11. $S_{21}$ parameter measured from measurement process.**

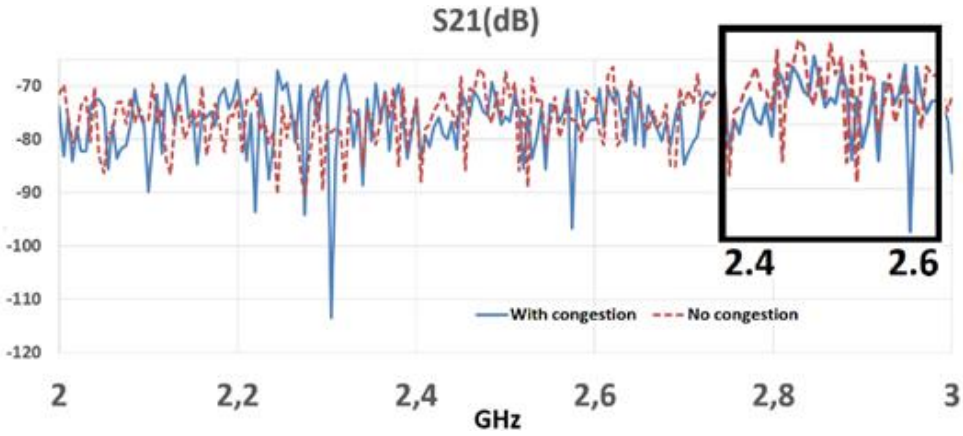


## IV. CONCLUSION

Deaths due to cardiovascular congestion are one of the most common causes of death in the world. Methods for detecting conventional cardiovascular congestion are performed with a surgical intervention or exposure to high-frequency rays. As an alternative to this situation, in this study, there is an alternative solution for the detection of cardiovascular congestion yet at the initial level. In the literature, by using the microstrip patch antenna structures which are widely used in biomedical areas, the differences in the scattering parameters are applied with the help of application and the changes in the electromagnetic field values with the help of simulations. Phantom prescriptions used in the application are obtained from the literature. The heart structure, which is designed during the simulations, is carried out by introducing the different electrical properties of the biological tissues in the literature.

Designed antenna structure radiates at 2.45 GHz. This antenna type has been selected because it has been the ISM band frequency zone. The substrate material used is determined as FR-4. This is because this substrate material is easily available.

Once the results are examined, the biggest difference for electric field values are showed for φ=0°. And the biggest loss difference is at $S_{11}$. For the scattering parameters, the magnitude of the loss difference for $S_{11}$ is important to detect congested heart vessel in the experiment.

As a result, it is shown that the antenna structure can show changes by acting in accordance with its purpose. By considering all these differences, it has been demonstrated that the designed antenna can be used for the detection of cardiovascular congestion yet at the initial stage.

**Conflict of interest**

There is no conflict to disclose.

## ACKNOWLEDGEMENT

This work was supported in part by the OYP Coordinator of Selcuk University with the project number: 2015-OYP-044."

## REFERENCES

[1] G. Lee, B. Garner, and Y. Li, "Development of a Human Body Phantom Model for Wireless Body Area Network Applications," Proc. 2019 Texas Symp. Wirel. Microw. Circuits Syst. WMCS 2019, pp. 2019–2021, 2019.

[2] J. Mao, W. Wang, G. Ding, and Z. Zhang, "Live Demonstration: Wearable Body Area Network System Based on Low Power Body Channel Communication," BioCAS 2019 - Biomed. Circuits Syst. Conf. Proc., vol. 11, no. 5, p. 100190, 2019.

[3] A. Saboor, A. Mustafa, R. Ahmad, M. A. Khan, M. Haris, and R. Hameed, "Evolution of wireless standards for health monitoring," IEMECON 2019 - 9th Annu. Inf. Technol. Electromechanical Eng. Microelectron. Conf., pp. 268–272, 2019.

[4] A. Sabban, "Small New Wearable Antennas for IOT, Medical and Sport Applications," 13th Eur. Conf. Antennas Propagation, EuCAP 2019, no. EuCAP, 2019.

[5] A. Quddious, P. Vryonides, S. Nikolaou, M. A. Antoniades, and M. A. B. Abbasi, "Through-body Communication Measurements Using Wearable and Implantable Sensor Antennas," Proc. 2019 Antennas Des. Meas. Int. Conf. ADMInC 2019, pp. 53–57, 2019.

[6] I. A. Shah, M. Zada, and H. Yoo, "Design and Analysis of a Compact-Sized Multiband Spiral-Shaped Implantable," vol. 67, no. 6,

pp. 4230–4234, 2019.
[7] T. S. Institution, "Ölüm Nedeni İstatistikleri, 2018 (Death Causes Statistics)," Turkey Statistical Institution Newsletter, 2019.
[8] F. H. Pratt, "THE NUTRITION OF THE HEART THROUGH THE VESSELS OF THEBESIUS AND THE CORONARY VEINS," Am. J. Physiol. Content, vol. 1, no. 1, pp. 86–103, Jan. 1898.
[9] J. L. Sullivan, "IRON AND THE SEX DIFFERENCE IN HEART DISEASE RISK," Lancet, vol. 317, no. 8233, pp. 1293–1294, Jun. 1981.
[10] R. Top, "A transmitter microstrip antenna design and application towards the detection of heart disease parameters," Selcuk University, 2017.
[11] R. Çalışkan, S. S. Gültekin, D. Uzer, and Ö. Dündar, "A Microstrip Patch Antenna Design for Breast Cancer Detection," Procedia - Soc. Behav. Sci., vol. 195, pp. 2905–2911, Jul. 2015.
[12] R. Top, S. S. Gültekin, and D. Uzer, "Evaluation of Electromagnetic Field Data of a Designed Microstrip Patch Antenna Structure According to Type of Substrate Materials and Their Thicknesses," Mater. Today Proc., vol. 18, pp. 1910–1917, 2019.
[13] H. Li, S. Sun, B. Wang, and F. Wu, "Design of Compact Single-Layer Textile MIMO Antenna for Wearable Applications," IEEE Trans. Antennas Propag., vol. 66, no. 6, pp. 3136–3141, 2018.
[14] S. A. Rezaeieh, A. Zamani, K. S. Bialkowski, and A. M. Abbosh, "Foam Embedded Wideband Antenna Array for Early Congestive Heart Failure Detection with Tests Using Artificial Phantom with Animal Organs," IEEE Trans. Antennas Propag., vol. 63, no. 11, pp. 5138–5143, Nov. 2015.
[15] R. Top, S. S. Gültekin, and D. Uzer, "Modeling congestion of vessel on rectangular microstrip antenna and evaluating electromagnetic signals," in 2017 25th Signal Processing and Communications Applications Conference (SIU), 2017, pp. 1–4.
[16] M. Nalam, N. Rani, and A. Mohan, "Biomedical Application of Microstrip Patch Antenna," Int. J. Innov. Sci. Mod. Eng., vol. 2, no. 6, pp. 6–8, 2014.
[17] E. Y. Chow, Y. Ouyang, B. Beier, W. J. Chappell, and P. P. Irazoqui, "Evaluation of cardiovascular stents as antennas for implantable wireless applications," IEEE Trans. Microw. Theory Tech., vol. 57, no. 10, pp. 2523–2532, Oct. 2009.
[18] E. F. Lincoln, "Heart Size," Circ. Res. An Off. J. Am. Hear. Assoc., vol. 39, no. 3, pp. 297–303, Sep. 1976.
[19] K. Ouerghi, N. Fadlallah, A. Smida, R. Ghayoula, J. Fattahi, and N. Boulejfen, "Circular antenna array design for breast cancer detection," 2017 Sensors Networks Smart Emerg. Technol. SENSET 2017, vol. 2017-Janua, no. 1, pp. 1–4, 2017.
[20] M. Z. Mahmud, M. T. Islam, N. Misran, S. Kibria, and M. Samsuzzaman, "Microwave imaging for breast tumor detection using uniplanar AMC Based CPW-fed microstrip antenna," IEEE Access, vol. 6, pp. 44763–44775, 2018.
[21] M. R. Karim, X. Yang, and M. F. Shafique, "On Chip Antenna Measurement: A Survey of Challenges and Recent Trends," IEEE Access, vol. 6, pp. 20320–20333, 2018.
[22] S. Shekhawat, P. K. Jain, B. R. Sharma, V. K. Saxena, and D. Bhatnagar, "An Off-diagonal Feed Elliptical Patch Antenna with Ring Shaped Slot in Ground Plane for Microwave Imaging of Breast," J. Nano- Electron. Phys., vol. 12, no. 1, pp. 1008-1-1008–4, 2020.
[23] M. A. Rahaman and Q. D. Hossain, "Design of a miniature microstrip wide band antenna for on-body biomedical telemetry," in Proceedings of the International Conference on Smart Systems and Inventive Technology, ICSSIT 2018, 2018, pp. 141–144.
[24] R. Raihan, M. S. Alam Bhuiyan, R. R. Hasan, T. Chowdhury, and R. Farhin, "Awearable microstrip patch antenna for detecting brain cancer," in 2017 IEEE 2nd International Conference on Signal and Image Processing, ICSIP 2017, 2017, vol. 2017-Janua, pp. 432–436.
[25] Z. J. Yang and S. Xiao, "A wideband implantable antenna for 2.4 GHz ISM band biomedical application," in 2018 IEEE International Workshop on Antenna Technology, iWAT2018 - Proceedings, 2018, pp. 1–3.
[26] C. Gabriel, "Compilation of the Dielectric Properties of Body Tissues at RF and Microwave Frequencies.," Environ. Heal., vol. Report No., no. June, p. 21, 1996.
[27] T. Yilmaz, R. Foster, and Y. Hao, "Broadband tissue mimicking phantoms and a patch resonator for evaluating noninvasive monitoring of blood glucose levels," IEEE Trans. Antennas Propag., vol. 62, no. 6, pp. 3064–3075, 2014.
[28] R. I. H. A.Kahwaji, H.Arshad, S.Sahran, A.G. Garba, "Hexagonal Microstrip Patch Antenna Simulation for Breast Cancer Detection," -, vol. 5, no. 1, pp. 1–4, 2016.
[29] R. Top, Y. Ünlü, S. S. Gültekin, and D. Uzer, "Microstrip antenna design with circular patch for skin cancer detection," Adv. Electromagn., vol. 8, no. 2, pp. 71–76, 2019.
[30] P. M. Meaney, T. Zhou, D. Goodwin, A. Golnabi, E. A. Attardo, and K. D. Paulsen, "Bone Dielectric Property Variation as a Function of Mineralization at Microwave Frequencies," Int. J. Biomed. Imaging, vol. 2012, 2012.
[31] J. T. Dodge, B. G. Brown, E. L. Bolson, and H. T. Dodge, "Lumen diameter of normal human coronary arteries: Influence of age, sex, anatomic variation, and left ventricular hypertrophy or dilation," Circulation, vol. 86, no. 1, pp. 232–246, 1992.
[32] D. M. Pozar et al., "Mikrodalga mühendisliği," 2012, p. 661.
[33] C. A. Balanis, "Anten teorisi : Analiz ve Tasarım," 3rd ed., Nobel Akademik Yayıncılık, 2013, p. 843.
[34] P. B. Samal, P. Jack Soh, and Z. Zakaria, "Compact and Wearable Microstrip-based Textile Antenna with Full Ground Plane Designed for WBAN-UWB 802.15.6 Application," in 2019 13th European Conference on Antennas and Propagation (EuCAP), 2019, pp. 1–4.
[35] M. A. Rahaman and Q. Delwar Hossain, "Design and overall performance analysis of an open end slot feed miniature microstrip antenna for on-body biomedical applications," in 1st International Conference on Robotics, Electrical and Signal Processing Techniques, ICREST 2019, 2019, pp. 200–204.
[36] R. Li, Y. X. Guo, B. Zhang, and G. Du, "A Miniaturized Circularly Polarized Implantable Annular-Ring Antenna," IEEE Antennas Wirel. Propag. Lett., vol. 16, pp. 2566–2569, Jul. 2017.
[37] D. Nikolayev, W. Joseph, A. Skrivervik, M. Zhadobov, L. Martens, and R. Sauleau, "Dielectric-Loaded Conformal Microstrip Antennas for Versatile In-Body Applications," IEEE Antennas Wirel. Propag. Lett., vol. 18, no. 12, pp. 2686–2690, Dec. 2019.
[38] L. Marnat, M. H. Ouda, M. Arsalan, K. Salama, and A. Shamim, "On-chip implantable antennas for wireless power and data transfer in a glaucoma-monitoring SoC," IEEE Antennas Wirel. Propag. Lett., vol. 11, pp. 1671–1674, 2012.
[39] C. Liu, Y. X. Guo, and S. Xiao, "Compact dual-band antenna for implantable devices," IEEE Antennas Wirel. Propag. Lett., vol. 11, pp. 1508–1511, 2012.
[40] C. Schmidt, F. Casado, A. Arriola, I. Ortego, P. D. Bradley, and D. Valderas, "Broadband UHF implanted 3-D conformal antenna design and characterization for in-off body wireless links," IEEE Trans. Antennas Propag., vol. 62, no. 3, pp. 1433–1444, 2014.
[41] A. D. Canonsburg, "HFSS Help," no. January, 2020.